Heavy neutron star phenomenology with an *H* dibaryon

Jesper Leong ,* Pierre A. M. Guichon , and Anthony W. Thomas
CSSM and ARC Centre of Excellence for Dark Matter Particle Physics, Department of Physics, Adelaide University, 5005 Adelaide, SA, Australia

(Received 8 April 2025; revised 29 September 2025; accepted 24 November 2025; published 28 January 2026)

The equation of state for dense nuclear matter in β equilibrium is explored including the possibility of a doubly strange H particle. Consistent with experimental constraints, the mass of the H in free space is taken to be near the $\Lambda\,\Lambda$ threshold. Within the quark-meson coupling model, which we use, no new parameters are required to describe the interaction between the H dibaryon and the other baryons. Compared with the case where only octet baryons are included, the maximum mass is only slightly reduced and the tidal deformability is essentially unchanged with this addition. In heavy neutron stars the H is abundant and extends nearly 6 km from the center of the star.

DOI: 10.1103/qs6f-1css

I. INTRODUCTION

New observations by NICER and the gravitational wave detectors make this an exciting time to study neutron stars (NS). Theoretical predictions which can be compared with these observations are hampered by our lack of understanding of matter at the extreme densities expected in these stars. Apart from the usual suspects, namely neutrons, protons, electrons and muons, one expects to find hyperons in the heavier stars and many authors have suggested other exotic particles may also appear; such as Δ baryons and dibaryons. There is also a possibility that the cores of the heavier stars may contain deconfined quarks and gluons.

Our focus is the potential role of an H dibaryon. This particle with quantum numbers spin and isospin zero, $B = 2$ and $S = -2$, was first proposed in 1977 as a deeply bound, exotic six-quark bag [1]. This inspired a large number of experiments aimed at finding this particle with negative results [2–8]. A particularly interesting experimental search for the H involves the examination of double Λ hypernuclei [9,10]. Here, a nucleus is formed with two Λ hyperons in an emulsion. If the H were deeply bound, the double Λ hypernucleus should decay into the original nucleus plus the H dibaryon. A few double Λ nuclei have been reported through Ξ capture; ${}^{10}_{\Lambda\Lambda}$Be [11,12], or interpreted as ${}^{13}_{\Lambda\Lambda}$B [13–15], and ${}^{6}_{\Lambda\Lambda}$He [7,16]. No such decay of $\Lambda\,\Lambda$ nuclei has been found, ruling out a deeply bound H. The NAGARA event at J-PARC (${}^{6}_{\Lambda\Lambda}$He) yields the most stringent constraint, namely, $M_H > 2224$ MeV [7].

While disappointing, the absence of a deeply bound H is consistent with the analysis of Mulders and Thomas [17], who showed that the larger size of the six-quark bag would reduce the pion self-energy leading to a mass prediction around the mass of two Λ hyperons. Uncertainties in that calculation meant that one could not be sure whether the H would be slightly bound or within a few 10s of MeV of that threshold.

Lattice quantum chromodynamics (QCD) calculations from the HAL [18] and NPLQCD [19] collaborations found a bound H close to the $\Lambda\,\Lambda$ threshold but with heavy u and d quarks. This motivated studies of the extrapolation to the physical u and d masses. For example, Shanahan *et al.* [20] used a chiral extrapolation to show that if it is indeed an exotic six-quark state the H is unbound by about 26 ± 11 MeV. If this is the case, one might expect that in dense matter in β equilibrium the H might appear soon after the Λ hyperon. Then the H might well exist inside the cores of heavier NS where the central core density is many times the saturation density of normal nuclear matter [21].

The temperature of NS is so low that it is natural to assume that it is below the critical temperature for Bose-Einstein condensation of the H particles. In the condensate all the particles are in the lowest state and therefore the kinetic energy is so low that it can barely resist to any attractive H-H interaction. The condensate then may collapse. However, this instability is unlikely in the H system because, at the density where the H can appear, the attractive H-H interaction due to σ exchange is balanced by the repulsive ω exchange [22]. Moreover in the quark-meson coupling (QMC) model that we use here the scalar polarizability effect reduces the σ-H coupling at high density. This is one more support to the H condensate hypothesis.

The early calculations of the role of the H in NS generally worked with the hypothesis that it was deeply bound. Furthermore, the strength of its coupling to the relativistic mean fields was not well understood. Typically, the ω coupling is fixed, which may be achieved by counting the number of nonstrange quarks [23], while the strength of the σ coupling was varied subject to the constraint that the H does not appear at ordinary saturation density. In one study the potential of the H at saturation was slightly attractive [23]. This is in contrast to a more recent study which suggested that a more repulsive interaction

*Contact author: jesper.leong@adelaide.edu.au

is necessary for the H if one is to generate sufficiently heavy stars [24].

Here, we consider the role of the H dibaryon using the QMC model, which has been successfully applied to heavy NS, even when hyperons are included [25–28]. The uniqueness of QMC stems from the coupling of the mesons directly to the confined quarks, leading to important changes in the structure of the baryons in-medium [29,30]. While the model was originally based upon the MIT bag model [31], similar features have been demonstrated within the Nambu–Jona-Lasinio (NJL) model [32–34]. Because it is the couplings of the mesons to the light quarks which are fundamental to this approach, the meson couplings to *all* hadrons are known for a given model of baryon structure *with no new parameters*. In particular, the meson couplings to the H dibaryon are not free parameters. In contrast with the situation for Λ hypernuclei, there have been very few observations of Ξ hypernuclei. In any case, the QMC predictions of the binding energies of the known hypernuclei are in reasonable agreement with data [35–38]. The advantage of using QMC to model the H is that there is no *a posteriori* fitting of the meson couplings of the H to fit NS observations. Either the H exists in NS and matches heavy NS observations, or it is not present in heavy NS.

In Sec. II we summarize the additions to the published QMC formalism necessary to include the H dibaryon. The results for the equation of state (EoS) and the properties of NS are described in Sec III, while Sec. IV presents some concluding remarks.

II. H DIBARYON IN THE QMC EQUATION OF STATE AND PARAMETRIZATIONS

A comprehensive review of the QMC model may be found in Refs. [25,29]. The QMC EoS, and its parametrizations, are provided in Ref. [27]. There we included a phenomenological "overlap" term to model possible short-distance repulsion at high densities not accounted for by the ω mean field. The QMC couplings are set to reproduce $n_0 = 0.16\ \text{fm}^{-3}$, $E_B/A = -15.8$ MeV, and $S = 30$ MeV. The slope of the symmetry energy and incompressibility are calculated to be 53 MeV and 260 MeV, respectively.

In this model the coupling of the baryon to the scalar mean field yields an effective mass which can be parametrized in terms of σ [38] [see Eq. (1)]:

$$M_f^*(\sigma) = M_f - w_f g_\sigma \sigma + \tilde{w}_f \frac{d}{2}(g_\sigma \sigma)^2. \tag{1}$$

Here g_σ (g_ω) is the free space coupling of the σ (ω) meson to the nucleon. The flavor dependent weightings, w_f and $\tilde{w}_f$, depend on the choice of R_N^{free}, the MIT bag radius in free space [38]. $R_N^{\text{free}} = 1.0$ fm is used here. The number of nonstrange quarks in the H dibaryon is twice that in the Λ. Since the scalar field in the QMC model couples only to the light quarks, the weightings w_H and $\tilde{w_H}$ are approximatively twice that of the Λ hyperon. The nonlinear term in Eq. (1) is a feature of QMC related to the response of the internal structure of the baryon to the applied scalar field. It is the origin of the many body force, with its strength encoded by the scalar polarizability, d.

This scalar polarizability is sensitive to R_N^{free} but to a good approximation the bag radius is the same for all baryons in the octet. However, because of the increase in the number of confined quarks in the H dibaryon, Mulders and Thomas found an increase by around 20% in the free bag radius for the H particle [17]. Here, we take $R_H = 1.2 \times R_N^{\text{free}}$. Thus the in-medium mass of the H particle is

$$\begin{aligned} M_H^* = M_H &- 2 \times [0.6672 + 0.04638 R_H - 0.0022 {R_H}^2] g_\sigma \sigma \\ &+ 2 \times [0.00146 + 0.0691 R_H - 0.00862 {R_H}^2](g_\sigma \sigma)^2. \end{aligned} \tag{2}$$

The only free parameter when incorporating the H into QMC is therefore its free mass, M_H. As discussed in the previous section, this mass is currently unknown. The best experimental lower bound suggests that it cannot be bound by more than about 10 MeV with respect to the $\Lambda\,\Lambda$ threshold. M_H is given in Eq. (3):

$$M_H = 2M_\Lambda - B_H. \tag{3}$$

We presume that the H is unbound and use as guidance the result from Shanahan *et al.* that $B_H = -26 \pm 11$ MeV [20].

The Lagrangian density for the H dibaryon is

$$\mathcal{L}_D = \mathcal{D}_\mu^* H^* \mathcal{D}^\mu H - {M_H^*}^2 H^* H, \tag{4}$$

where $\mathcal{D}_\mu = \partial_\mu + i g_{\omega,H} \omega_\mu$ includes the coupling to the ω vector field [22,23]. Since H is a boson with zero isospin the ρ does not couple to it.

The Euler-Lagrange equation is then

$$\left(\mathcal{D}_\mu \mathcal{D}^\mu + {M_H^*}^2\right) H = 0. \tag{5}$$

The H particle is a boson and hence forms a condensate with $\vec{k} = 0$. At mean-field level one can show that for an s-wave condensate the chemical potential is

$$\mu_H = M_H^* + g_{\omega,H}\omega. \tag{6}$$

It follows that the density is simply

$$n_H = 2 M_H^* H^* H. \tag{7}$$

The H modifies the mean-fields as follows:

$${m_\sigma}^2 \sigma + \lambda_3 \frac{{g_\sigma}^3}{2} \sigma^2 = \sum_f n_f^s - \frac{\partial M_H^*}{\partial \sigma} n_H, \tag{8}$$

$${m_\omega}^2 \omega = \sum_f g_{\omega,f} n_f^v + g_{\omega,H} n_H. \tag{9}$$

Here, $\lambda_3 = 0.02\ \text{fm}^{-1}$ is the coefficient of the self-interaction of the σ field, which is needed to reproduce the giant monopole resonance energies in finite nuclei [42]. n^s and n^v are the scalar and vector densities, respectively, and the summation is over n, p, Λ, Ξ^0, and Ξ^-. The last terms in Eqs. (8) and (9) is the contributions of the H to the respective mean fields [23]. Finally, the H contribution to the energy is

$$\varepsilon_H = 2 {M_H^*}^2 H^* H = M_H^* n_H. \tag{10}$$

We note that the theory outlined above is thermodynamically consistent [22,23,43]. In Ref. [23] the authors observed that there is no direct contribution from the H to the pressure. However, the pressure does change indirectly because of the

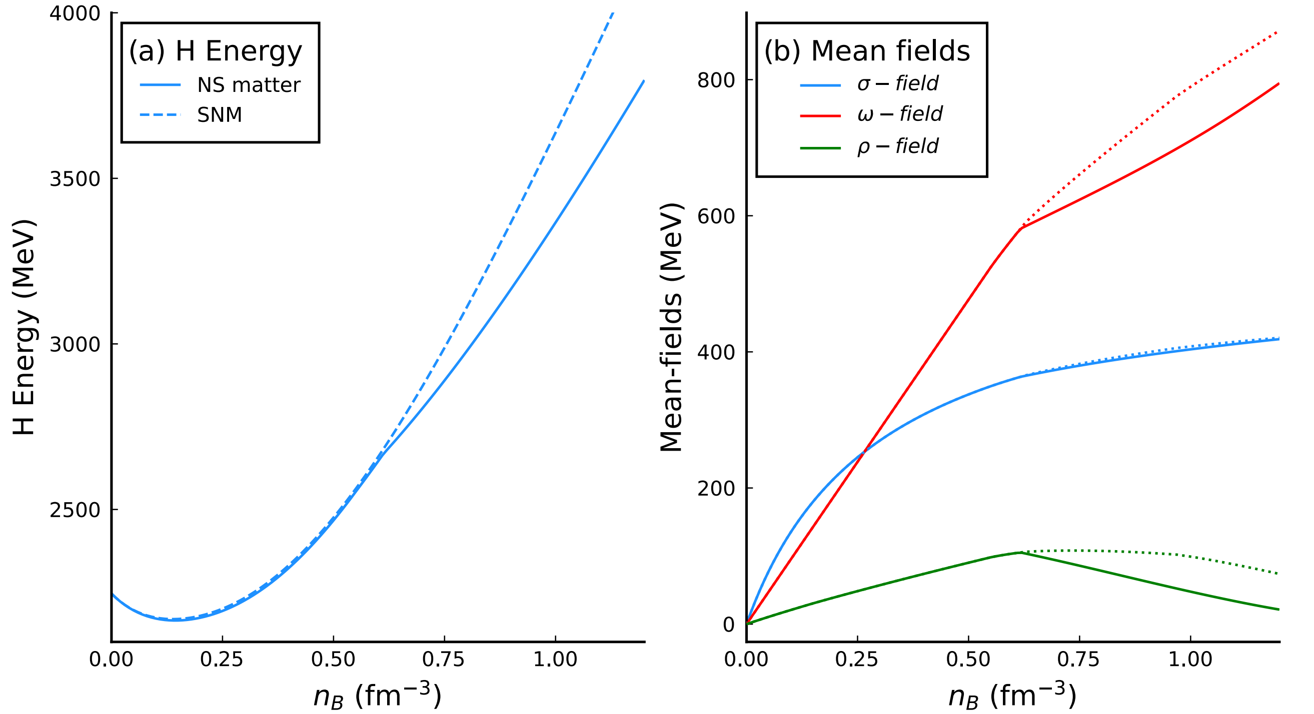

FIG. 1. In (a) the energy of the H particle in SNM (dashed line) and NS matter at β equilibrium (solid line) are presented. In (b) the mean fields with nucleon couplings in NS matter are shown with (solid line) and without (dotted line) the H dibaryon. Since the neutron has isospin of $-1/2$, the isovector ρ is inverted to present positive values. Both results in this figure are for $M_H = 2247$ MeV.

modifications of the mean-fields, as we can see from Eqs. (8) and (9).

As discussed in detail in Ref. [27], we account for the potential additional short-distance repulsion that may be present at high densities by incorporating the overlap term. This is dependent on the total number density, $n_B = \sum_f n_f + 2n_H$. In this case the H does change the pressure through both the modification of the mean fields and the overlap mechanism. Tamagaki suggested that the hard-core radius of the H dibaryon should be between 0.5–0.7 fm [21]. The range parameter in the overlap model used here is consistent with this. For simplicity we presume that the H has the same hard-core radius as the rest of the baryons. In Appendix the reader will find a brief additional discussion on the short-distance repulsion interaction incorporated here, which is complimentary to that presented in Ref. [27].

III. RESULTS

In Fig. 1(a) the energy of the H dibaryon is presented in the case of symmetric nuclear matter (SNM) and NS matter in β equilibrium. The minimum energy of the H is found close to the saturation density of SNM. The H is bound by 82 MeV in NS matter and 77 MeV in SNM. The difference is accounted for by the small change in the σ field associated with the additional neutrons in NS matter [see Eq. (8)]. For reference, the Λ is bound by around 38 MeV. The solid line representing the energy of the H in matter in β equilibrium, as shown in Fig. 1(a), starts to diverge from SNM when the H appears because of the modifications of the mean fields.

Figure 1(b) shows the magnitudes of the mean fields experienced by nucleons in NS matter. The H particle appears at around 0.6 fm^{-3} [see Fig. 3(a)] and is subject to an overall repulsive interaction which allows the H condensate to be stable. After the H appears the strength of the ω field is weakened in accordance with Eq. (9). The weakening to the isovector vector ρ, which the H does not couple to, is primarily caused by the decrease in neutron density. In Fig. 2 we show the effective mass of the H, M_H^*, which is reduced in response to the scalar attraction.

The H particle is electrically neutral but carries baryon number 2. Thus, the only modification to β equilibrium is to

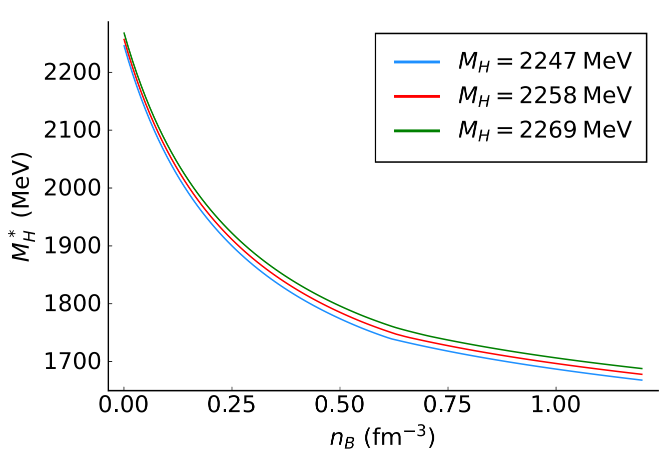

FIG. 2. The effective mass of the H as given by Eq. (2).

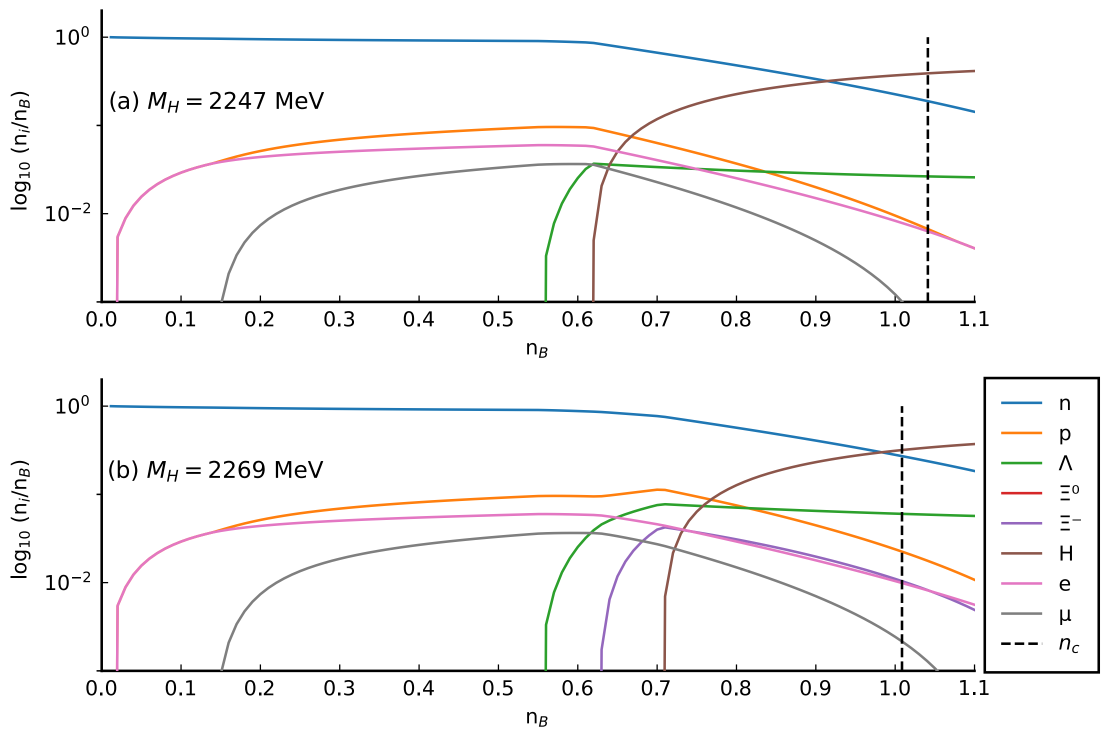

FIG. 3. Species fractions for β-stable matter. In (a) $M_H = 2247$ MeV and (b) $M_H = 2269$ MeV, we show the particle fractions as a function of total number density. n_c denotes the central number density for the maximum mass NS as depicted by the black dashed vertical line with the precise values listed in Table I. The lower free mass of the H in (a) means it appears before Ξ^-, which no longer appears in the EoS.

the conservation of baryon number. Figure 3 shows the species fractions for a) $M_H = 2247$ MeV and b) $M_H = 2269$ MeV. The H particle always appears after the Λ, given that we have chosen M_H such that H lies above the $\Lambda\,\Lambda$ threshold. The threshold density of the H is increased with increasing M_H. The H is in competition with the hyperons and besides a reduction in the abundance of the other baryons, the presence of the H increases the threshold density at which any new hyperon appears after the H. In this case, those hyperons are the Ξ^- and Ξ^0. Without the H, the Ξ^0 baryons were present in the QMC EoS at high densities [27] but once the H is included the Ξ^0 does not appear at all. For $M_H = 2247$ MeV, Ξ^- also does not appear. In Fig. 3 the central density for the maximum mass star is indicated by the black dashed line for $M_H = 2247$ MeV and 2269 MeV. Near this threshold the H is abundant, indicating that the cores of heavy NS may contain a sizable fraction of H-matter condensate. Figure 4 depicts the population of baryons and the H dibaryon in the interior of a maximum mass star for $M_H = 2258$ MeV. The maximum mass, radius and central energy density, pressure, and number density are located in Table I. The H particle is highly abundant in the center of the star and extends out to a radius of around 5.7 km.

The EoS is presented in Fig. 5(a). The low density EoS presented by Hempel and Schaffner-Bielich was used to accurately model the crustal regions of the NS [44,45]. The EoS for the case with no H is indicated with the dotted black line. As expected, the appearance of the hyperon and the H particle softens the EoS as each of their threshold densities are reached. The overlap interaction mitigates the softening of the EoS normally associated with hyperons due to the loss of neutron degeneracy pressure. The same is also true of the H.

As we see in Fig. 5(b), the presence of the H does slightly reduce the maximum mass predicted by the QMC model. Nevertheless, the maximum masses obtained with all three choices of M_H exceed $M_{NS} > 2.0\, M_\odot$ (see Table I). Although the choice of M_H changes the density at which the H dibaryon appears, there is no great reduction in the maximum mass of the NS, with a larger value of M_H yielding a smaller reduction in the maximum mass. We further note that with the H particle, the radius at maximum mass is larger. Larger choices for M_H correspond to larger radii at maximum mass.

In the past, canonical mass stars were thought to have a radius $R < 12$ km [46,47]. Recent NICER missions favor stiffer EoS with increased radii. PSR J0030 + 0451 has

TABLE I. The maximum mass (M_{NS}, $M_\odot$) and corresponding radius (R, km), for each choice of M_H (MeV) is presented along with the central number density (n_c, fm^{-3}), energy density (ε_c, MeV fm^{-3}), and pressure (P_c, MeV fm^{-3}). For reference, the case with no H dibaryon is presented at the top of the table [27].

M_H	M_{NS}	R	n_c	ε_c	P_c
–	2.12	10.94	1.03	537	1309
2247	2.07	11.02	1.04	489	1308
2258	2.08	11.11	1.02	467	1268
2269	2.10	11.12	1.01	467	1230

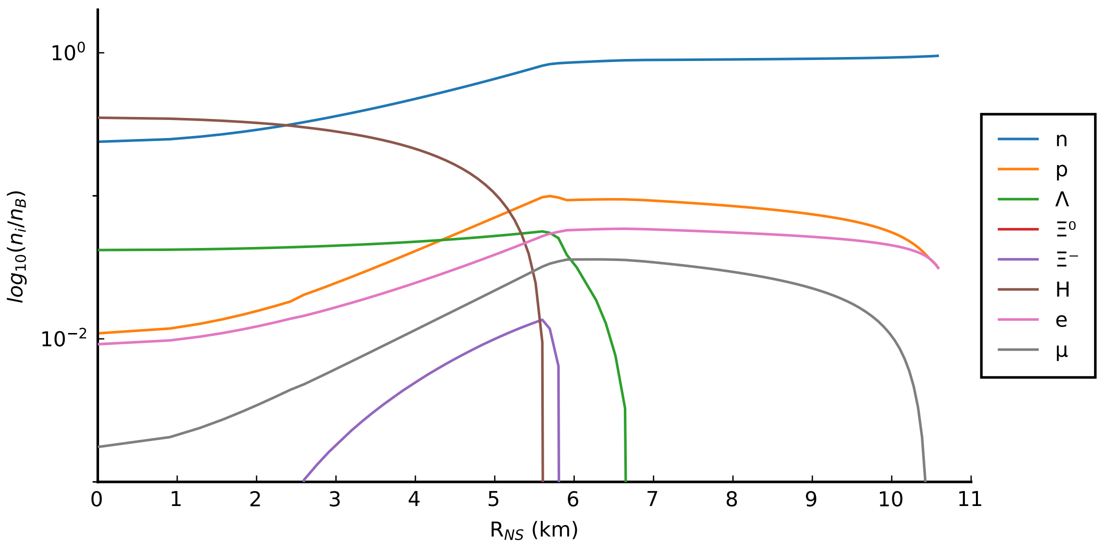

FIG. 4. Particle population within the interior core of a maximum mass NS when $M_H = 2258$ MeV. The species fractions is truncated at the crust-core boundary.

$M = 1.44^{+0.15}_{-0.14} M_\odot$ and $R = 13.02^{+1.24}_{-1.06}$ km [41] (Riley *et al.* is consistent with this [48]). The H particle modeled in QMC plays no role in low mass stars, but the particular QMC parametrizations to produce a heavy mass NS is consistent with the radius of low mass NS. For heavier mass stars, the radii found here are consistent with the observation of PSR J0740 + 6620, as depicted in Fig. 5(b) [40] (see also [49–53]). This mass is similar to that of the first heavy NS discovered, PSR J1614-2230 by Demorest *et al.* [54].

Potentially the heaviest known pulsar, PSR J0952-0607, has a mass of $M = 2.35 \pm 0.17 M_\odot$, at 1σ [39]. The central value would challenge all hyperonic QMC EoS, with or

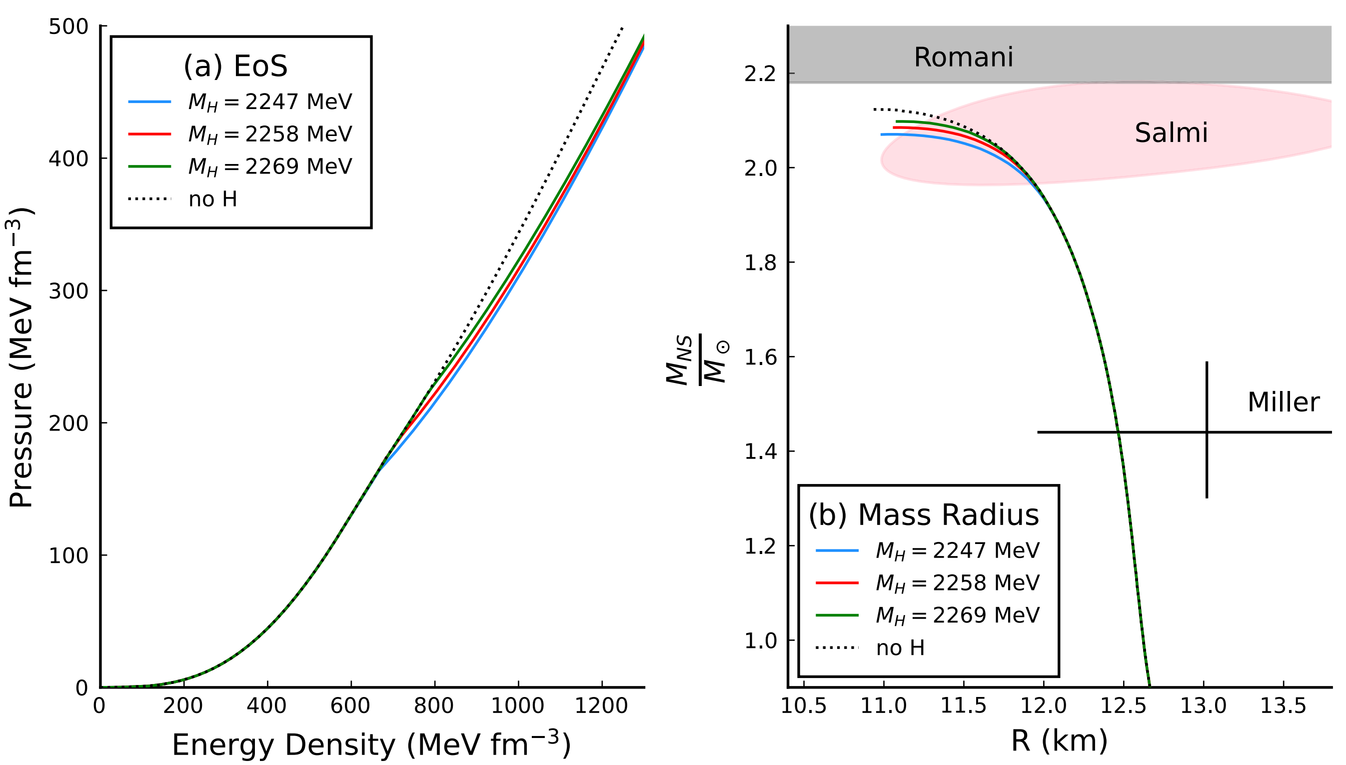

FIG. 5. (a) The QMC EoS for difference masses of H. In the dotted black line we show the EoS without the H dibaryon [27]. The curves begin to deviate once the H appears. (b) The resultant mass-radius curves calculated using the TOV equation. Romani *et al.* depicts the heaviest known NS, PSR J0952-0607 [39]. The observation of PSR J0740 + 6620 is extracted from analysis performed by Salmi *et al.* [40]. Miller *et al.* is the NICER estimation for the canonical mass star from PSR J0030 + 0451 [41].

without the H particle; see Table I, which also displays the central density, energy, and pressure for no H, and each choice of M_H at maximum mass. On the other hand, at 3σ the lower bound of the mass of PSR J0952-0607 is $2.09M_\odot$ [39]. PSR J0952-0607 is a rapidly rotating pulsar, spinning at approximately 700 Hz [55]. The Tolman-Oppenheimer-Volkoff (TOV) equation used here assumes a nonrotating or slowly rotating spherically symmetric NS. Because PSR J0952-0607 spins so rapidly, it can support additional mass, as well as an increase in equatorial radius. Although the spin is well below the Kepler limit (mass shedding), it is non-negligible with the rotation possibly requiring a 5–10 % correction to $M_{\rm TOV}$ [56,57]. Within the QMC model it has previously been demonstrated that it can yield a $2.22M_\odot$ star [28], which is not inconsistent with PSR J0952-0607. Given that the H particle only slightly reduces the maximum mass of a star, it is possible that PSR J0952-0607 may contain a bosonic H-particle core.

Finally around the canonical mass value, $M_{NS} = 1.4\ M_\odot$, QMC EoS does not contain any hyperons, or H, and therefore the tidal deformability for $\Lambda_{1.4} \approx 430$ remains the same as previously reported by Leong *et al.* [27].

IV. CONCLUSION

We have examined the effects on the EoS of dense matter in β equilibrium when one includes the possibility of an H dibaryon with mass somewhat higher than the $\Lambda\,\Lambda$ threshold. The QMC model was chosen because all the meson couplings to the H are predicted within the model, rather than being free parameters. The version of the model chosen successfully describes the binding energies, deformations, and charge radii of even-even nuclei across the periodic table [42,58], with just five parameters. It includes a term involving the scalar field cubed, which is necessary to describe the energies of the giant monopole resonances. Then, in order to generate stars with masses of order $2M_\odot$, one needs additional repulsion at densities well above nuclear matter density. Following Ref. [27], we use a phenomenological term which depends on the extent to which baryons overlap and with a strength chosen to yield heavy NS when octet hyperons are included. This term was chosen so as not to change the properties of finite nuclei and the EoS it yields was shown (see the Appendix) to be consistent with constraints from heavy ion collisions.

The TOV equation was then solved to obtain the masses and radii of NS generated by the new EoS. When the H dibaryon is included in addition to the octet hyperons, it tends to slightly lower the central energy density and pressure for the heaviest stars. The maximum masses remain above $2\ M_\odot$. In addition, because the H dibaryon only appears well above three times the saturation density of nuclear matter, the successful predictions for tidal deformability reported in earlier work remain unchanged.

We have shown that including the H dibaryon yields results which are compatible with observations of heavy NS and the observed tidal deformability. The mass-radius relation is not altered sufficiently that one could distinguish its presence, as opposed to a star containing only octet baryons. Nevertheless, it is remarkable that if the H dibaryon does exist the particle content of the core of a heavy NS will be very different, with the H dibaryon being the dominant component other than neutrons in regions where the density exceeds $3-4n_0$.

ACKNOWLEDGMENTS

This work was supported by the Adelaide University and the Australian Research Council through a grant to the ARC Centre of Excellence for Dark Matter Particle Physics (CE200100008) and DP230101791 (A.W.T.).

DATA AVAILABILITY

The data that support the findings of this article are openly available [59].

APPENDIX: PNM AND SNM HEAVY ION CONSTRAINTS

The phenomenological overlap term from Ref. [27] is independent of the particle species. Because of this the H particle has a direct influence on the pressure at high densities through the short-distance repulsion phenomenological term. The overlap term is

$$E_0 n_B \exp\left\{-\left(\frac{{n_B}^{-1/3}}{b}\right)^2\right\}. \tag{A1}$$

$E_0 = 5500$ MeV and $b = 0.5$ fm are used here, which has been chosen to only affect the EoS at suprasaturation densities (see [27] for details).

Figure 6 displays the EoS for pure neutron matter (PNM) and symmetric nuclear matter (SNM), along with heavy ion collision analysis from Refs. [60] and [61]. Heavy ion collision data is difficult to interpret given the model dependent uncertainty in the density and the high temperatures reached. Furthermore, the timescales involved do not allow for β equilibrium to be established; unlike the formation of NSs. Nevertheless, the QMC EoS is consistent with both Ref. [60] and earlier work of Ref. [61].

Note that in Refs. [52] and [62], analysis from NS observations, favor a stiffer EoS. NICER measurements of PSR J0437-4715 is $M = 1.418 \pm 0.037M_\odot$ and $R = 11.36^{+0.95}_{0.63}$ [63]. Both GW 170817 and PSR J0437-4715 favor a soft EoS, whilst the existence of NS with masses greater than $2.0M_\odot$ favors a stiff EoS. It is difficult to reconcile both of these within a single EoS. However, one could demand that at low/intermediate densities the EoS is soft to satisfy low radius canonical mass stars before stiffening greatly at higher densities to support heavy mass stars. A phenomenological overlap term, such as that in Eq. (A1) models this scenario. In particular, it is suggested that when the baryons begin to overlap at high densities, the quark cores may generate additional strong repulsion brought about by the Pauli exclusion principle and a multiquark environment. The QMC model has five model parameters plus an additional two when using the phemenological overlap interaction to model high density repulsion. This is in contrast, for example, to Kumar *et al.* who constructed nucleon-only EoS using up to 12 model

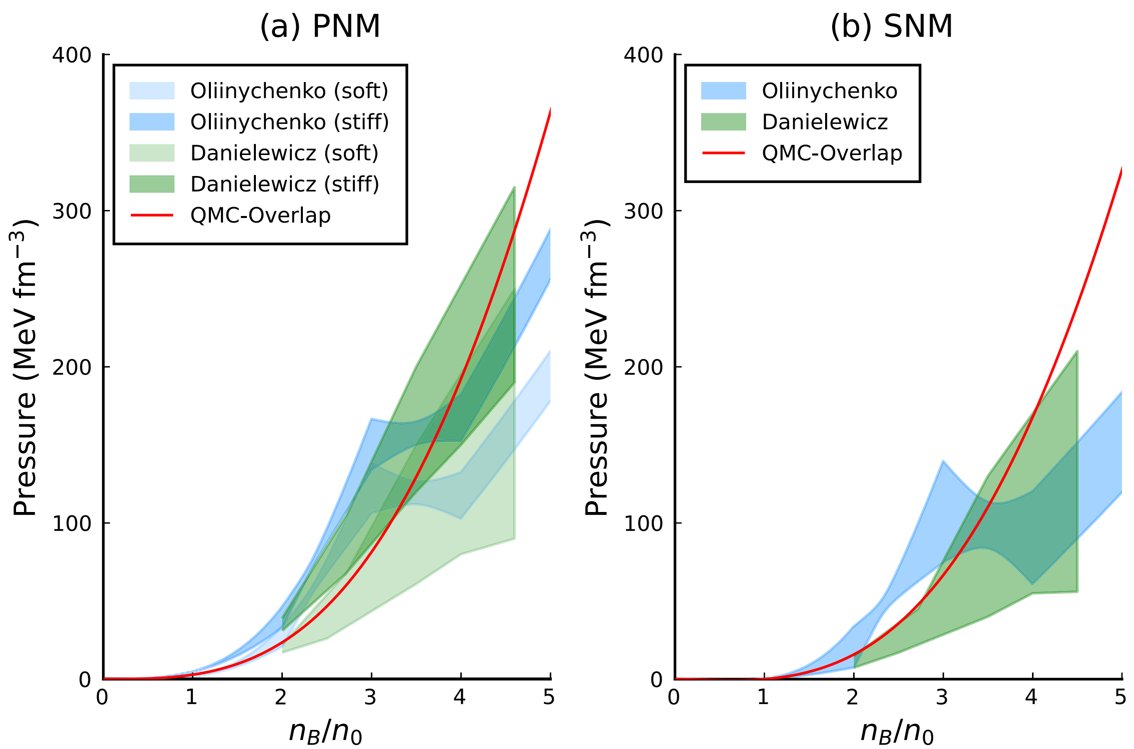

FIG. 6. (a) PNM and (b) SNM EoS from QMC with the overlap interaction used here is shown in red. References [60] and [61] are shown in green (Oliinychenko) and blue (Danielewicz), respectively.

parameters [64], which may be even stiffer than the SNM and PNM EoS from Danielewicz *et al.* [61]. Our intention here is not to explore the parametrization of the overlap interaction but the possible role of the H at supranuclear densities.

[1] R. L. Jaffe, Perhaps a stable dihyperon, Phys. Rev. Lett. **38**, 195 (1977); **38**, 617(E) (1977).
[2] A. Gal, Hypernuclear constraints on the existence and lifetime of a deeply bound h dibaryon, Phys. Lett. B **857**, 138973 (2024).
[3] H. Ejiri, E. Takasugi, T. Kishimoto, H. Ohsumi, J. Tanaka, and A. Kashitani, Search for the *H* dihyperon by double weak decay of nuclei, Phys. Lett. B **228**, 24 (1989).
[4] C. B. Dover, Strange dibaryon production in relativistic heavy ion collisions, Nuovo Cimento A **102**, 521 (1989).
[5] T. Iijima, *et al.*, (K^-, K^+) reaction on nuclear targets at $P_K =$ 1.65 G, Nucl. Phys. A **546**, 588 (1992).
[6] R. W. Stotzer, *et al.*, Search for H dibaryon in $^3He(K^-, k^+)Hn$, Phys. Rev. Lett. **78**, 3646 (1997).
[7] H. Takahashi, *et al.*, Observation of a $^{6}_{\Lambda\Lambda}He$ double hypernucleus, Phys. Rev. Lett. **87**, 212502 (2001).
[8] C. J. Yoon, *et al.*, Search for the H-dibaryon resonance in ^{12}C$(K-, k^+\Lambda\Lambda X)$, Phys. Rev. C **75**, 022201 (2007).
[9] T. F. Carames and A. Valcarce, The renewed challenge of the H dibaryon, Int. J. Mod. Phys. E **22**, 1330004 (2013).
[10] T. Sakai, K. Shimizu, and K. Yazaki, H dibaryon, Prog. Theor. Phys. Suppl. **137**, 121 (2000).
[11] M. Danysz, *et al.*, Observation of a double hyperfragment, Phys. Rev. Lett. **11**, 29 (1963).
[12] M. Danysz, *et al.*, The identification of a double hyperfragment, Nucl. Phys. **49**, 121 (1963).
[13] Y. Yamamoto, H. Takaki, and K. Ikeda, Newly observed double lambda hypernucleus and Λ-Λ interaction, Prog. Theor. Phys. **86**, 867 (1991).
[14] S. Aoki, *et al.*, Direct observation of sequential weak decay of a double hypernucleus, Prog. Theor. Phys. **85**, 1287 (1991).
[15] C. B. Dover, D. J. Millener, A. Gal, and D. H. Davis, Interpretation of a double hypernucleus event, Phys. Rev. C **44**, 1905 (1991).
[16] D. J. Prowse, Λ-Λ He-6 double hyperfragment, Phys. Rev. Lett. **17**, 782 (1966).
[17] P. J. Mulders and A. W. Thomas, Pionic corrections and multiquark bags, J. Phys. G **9**, 1159 (1983).
[18] T. Inoue, S. Aoki, T. Doi, T. Hatsuda, Y. Ikeda, N. Ishii, K. Murano, H. Nemura, and K. Sasaki, Two-baryon potentials and *H*-dibaryon from 3-flavor lattice QCD simulations, Nucl. Phys. A **881**, 28 (2012).
[19] S. R. Beane, E. Chang, S. D. Cohen, W. Detmold, H. W. Lin, T. C. Luu, K. Orginos, A. Parreno, M. J. Savage, and A. Walker-Loud, Light nuclei and hypernuclei from quantum chromodynamics in the limit of SU(3) flavor symmetry, Phys. Rev. D **87**, 034506 (2013).
[20] P. E. Shanahan, A. W. Thomas, and R. D. Young, Updated analysis of the mass of the H dibaryon from lattice QCD, JPS Conf. Proc. **1**, 013028 (2014).

[21] R. Tamagaki, Implications of the H dihyperon in high density hadronic matter, Prog. Theor. Phys. **85**, 321 (1991).
[22] A. Faessler, A. J. Buchmann, M. I. Krivoruchenko, and B. V. Martemyanov, Dibaryons in nuclear matter, J. Phys. G **24**, 791 (1998).
[23] N. K. Glendenning and J. Schaffner-Bielich, Neutron star constraints on the H dibaryon, Phys. Rev. C **58**, 1298 (1998).
[24] X. Wu, L. Wang, H.-T. An, M. Ju, and H. Shen, Properties of H particle-admixed compact star, arXiv:2402.14288.
[25] J. Rikovska-Stone, P. A. M. Guichon, H. H. Matevosyan, and A. W. Thomas, Cold uniform matter and neutron stars in the quark-mesons-coupling model, Nucl. Phys. A **792**, 341 (2007).
[26] T. F. Motta, P. A. M. Guichon, and A. W. Thomas, On the sound speed in hyperonic stars, Nucl. Phys. A **1009**, 122157 (2021).
[27] J. Leong, T. F. Motta, A. W. Thomas, and P. A. M. Guichon, Dense nuclear matter with phenomenological short distance repulsion, Phys. Rev. C **108**, 015804 (2023).
[28] J. Leong, A. W. Thomas, and P. A. M. Guichon, Excluded volume effects on cold neutron star phenomenology, Nucl. Phys. A **1050**, 122928 (2024).
[29] P. A. M. Guichon, J. R. Stone, and A. W. Thomas, Quark-meson-coupling (QMC) model for finite nuclei, nuclear matter and beyond, Prog. Part. Nucl. Phys. **100**, 262 (2018).
[30] P. A. M. Guichon, K. Saito, E. N. Rodionov, and A. W. Thomas, The role of nucleon structure in finite nuclei, Nucl. Phys. A **601**, 349 (1996).
[31] A. Chodos, R. L. Jaffe, K. Johnson, and C. B. Thorn, Baryon structure in the bag theory, Phys. Rev. D **10**, 2599 (1974).
[32] W. Bentz and A. W. Thomas, The stability of nuclear matter in the Nambu-Jona-Lasinio model, Nucl. Phys. A **696**, 138 (2001).
[33] H. Mineo, W. Bentz, N. Ishii, A. W. Thomas, and K. Yazaki, Quark distributions in nuclear matter and the EMC effect, Nucl. Phys. A **735**, 482 (2004).
[34] I. C. Cloet, W. Bentz, and A. W. Thomas, Spin-dependent structure functions in nuclear matter and the polarized EMC effect, Phys. Rev. Lett. **95**, 052302 (2005).
[35] O. Hashimoto and H. Tamura, Spectroscopy of lambda hypernuclei, Prog. Part. Nucl. Phys. **57**, 564 (2006).
[36] K. Nakazawa, *et al.*, The first evidence of a deeply bound state of $\mathrm{Xi}^- - {}^{14}\mathrm{N}$ system, Prog. Theor. Exp. Phys. **2015**, 033D02 (2015).
[37] R. Shyam and K. Tsushima, Description of the recently observed hypernucleus ${}^{15}_{\Xi^-}\mathrm{C}$ within a quark-meson coupling model, arXiv:1901.06090.
[38] P. A. M. Guichon, A. W. Thomas, and K. Tsushima, Binding of hypernuclei in the latest quark-meson coupling model, Nucl. Phys. A **814**, 66 (2008).
[39] R. W. Romani, D. Kandel, A. V. Filippenko, T. G. Brink, and W. Zheng, PSR J0952-0607: The fastest and heaviest known galactic neutron star, Astrophys. J. Lett. **934**, L17 (2022).
[40] T. Salmi, *et al.*, The radius of the high-mass pulsar PSR J0740 6620 with 3.6 yr of NICER data, Astrophys. J. **974**, 294 (2024).
[41] M. C. Miller, *et al.*, PSR J0030 0451 mass and radius from *NICER* data and implications for the properties of neutron star matter, Astrophys. J. Lett. **887**, L24 (2019).
[42] K. M. L. Martinez, A. W. Thomas, J. R. Stone, and P. A. M. Guichon, Parameter optimization for the latest quark-meson coupling energy-density functional, Phys. Rev. C **100**, 024333 (2019).
[43] A. Faessler, A. J. Buchmann, M. I. Krivoruchenko, and B. V. Martemyanov, Nuclear matter with a Bose condensate of dibaryons in relativistic mean field theory, Phys. Lett. B **391**, 255 (1997).
[44] M. Hempel and J. Schaffner-Bielich, Statistical model for a complete supernova equation of state, Nucl. Phys. A **837**, 210 (2010).
[45] M. Hempel, T. Fischer, J. Schaffner-Bielich, and M. Liebendorfer, New equations of state in simulations of core-collapse supernovae, Astrophys. J. **748**, 70 (2012).
[46] M. Oertel, M. Hempel, T. Klähn, and S. Typel, Equations of state for supernovae and compact stars, Rev. Mod. Phys. **89**, 015007 (2017).
[47] F. Özel, D. Psaltis, T. Güver, G. Baym, C. Heinke, and S. Guillot, The dense matter equation of state from neutron star radius and mass measurements, Astrophys. J. **820**, 28 (2016).
[48] T. E. Riley, *et al.*, A *NICER* view of PSR J0030 +045 1: Millisecond pulsar parameter estimation, Astrophys. J. Lett. **887**, L21 (2019).
[49] H. T. Cromartie, *et al.*, Relativistic shapiro delay measurements of an extremely massive millisecond pulsar, Nat. Astron. **4**, 72 (2019).
[50] E. Fonseca, *et al.*, Refined mass and geometric measurements of the high-mass PSR J0740+6620, Astrophys. J. Lett. **915**, L12 (2021).
[51] T. E. Riley, *et al.*, A NICER view of the massive pulsar PSR J0740+6620 informed by radio timing and XMM-Newton spectroscopy, Astrophys. J. Lett. **918**, L27 (2021).
[52] M. C. Miller, *et al.*, The radius of PSR J0740+6620 from NICER and XMM-newton data, Astrophys. J. Lett. **918**, L28 (2021).
[53] G. Raaijmakers, S. K. Greif, K. Hebeler, T. Hinderer, S. Nissanke, A. Schwenk, T. E. Riley, A. L. Watts, J. M. Lattimer, and W. C. G. Ho, Constraints on the dense matter equation of state and neutron star properties from NICER's mass–radius estimate of PSR J0740+6620 and multimessenger observations, Astrophys. J. Lett. **918**, L29 (2021).
[54] P. Demorest, T. Pennucci, S. Ransom, M. Roberts, and J. Hessels, Shapiro delay measurement of a two solar mass neutron star, Nature (London) **467**, 1081 (2010).
[55] C. G. Bassa, *et al.*, LOFAR discovery of the fastest-spinning millisecond pulsar in the galactic field, Astrophys. J. Lett. **846**, L20 (2017).
[56] A. Konstantinou and S. M. Morsink, Universal relations for the increase in the mass and radius of a rotating neutron star, Astrophys. J. **934**, 139 (2022).
[57] Z. Wu, B. Biswas, and S. Rosswog, PSR J0952-0607: Probing the stiffest equations of state and r-mode suppression mechanisms, arXiv:2502.09200.
[58] K. M. L. Martinez, A. W. Thomas, P. A. M. Guichon, and J. R. Stone, Tensor and pairing interactions within the quark-meson coupling energy-density functional, Phys. Rev. C **102**, 034304 (2020).
[59] J. Leong, Heavy neutron star phenomenology with an H-dibaryon (2025), https://doi.org/10.7910/DVN/CLYS13.
[60] D. Oliinychenko, A. Sorensen, V. Koch, and L. McLerran, Sensitivity of au au collisions to the symmetric nuclear matter equation of state at 2–5 nuclear saturation densities, Phys. Rev. C **108**, 034908 (2023).

[61] P. Danielewicz, R. Lacey, and W. G. Lynch, Determination of the equation of state of dense matter, Science **298**, 1592 (2002).

[62] R. Essick, I. Tews, P. Landry, S. Reddy, and D. E. Holz, Direct astrophysical tests of chiral effective field theory at supranuclear densities, Phys. Rev. C **102**, 055803 (2020).

[63] D. Choudhury, *et al.*, A nicer view of the massive pulsar PSR J0740 + 6620 informed by radio timing and XMM-Newton spectroscopy, Astrophys. J. Lett. **971**, L20 (2024).

[64] R. Kumar, M. Kumar, V. Thakur, S. Kumar, P. Kumar, A. Sharma, B. K. Agrawal, and S. K. Dhiman, Observational constraint from the heaviest pulsar PSR J0952-0607 on the equation of state of dense matter in relativistic mean field model, Phys. Rev. C **107**, 055805 (2023).